Randomized Distributed Configuration Management of Wireless Networks: Multi-layer Markov Random Fields and Near-Optimality

Sung-eok Jeon and Chuanyi Ji, Senior Member, IEEE

arXiv:0809.1916v1 [cs.DC] 11 Sep 2008

***Abstract*—Distributed configuration management is imperative for wireless infrastructureless networks where each node adjusts locally its physical and logical configuration through information exchange with neighbors. Many algorithms have been developed with promising results in this area. However, two issues remain open. The first is the optimality, i.e., whether a distributed algorithm results in a near-optimal *network* configuration. The second is the complexity, i.e., whether a distributed algorithm scales gracefully with network size (N). We study these issues through modeling, analysis, and randomized distributed algorithms.**

Modeling defines the optimality. We first derive a global probabilistic model for a network configuration which characterizes jointly the statistical spatial dependence of a physical- and a logical-configuration. The model is a Gibbs distribution that results from internal network properties on node positions, wireless channels and interference; and external management constraints on physical connectivity, signal quality and configuration costs. We then show that a local model which approximates the global model is a two-layer Markov Random Field or a random bond model. The complexity of the local model is the communication range among nodes. The local model is near-optimal when the approximation error to the global model is within a given error bound. We analyze the trade-off between an approximation error and complexity, and derive sufficient conditions on the near-optimality of the local model. We show that when the power attenuation of a wireless channel is larger than 4, a node needs to communicate with more than $O(1)$ neighbors for a local model to be near optimal. For a slowly decaying channel with power attenuation less than 4, a node may need to communicate with more than $O(\sqrt[3]{N})$ neighbors to result in a bounded approximation error. The two-layer Markov Random Fields enable a class of randomized distributed algorithms that allow a node to self-configure based on information from its neighbors. The distributed algorithms are applied to examples of (a) forming a 1-connected physical topology, (b) configuring a logical topology that maximizes the spatial channel reuse, and (c) reconfiguring from failures, both sequentially and jointly. We validate the model, the analysis and the randomized distributed algorithms also through simulation.

I. Introduction

Wireless infrastructureless networks include sensor- and actor-networks, wireless mesh networks, and agent networks. Such networks are composed of a physical and a logical configuration (topology). A physical configuration is characterized by node positions and connectivity. A logical configuration is characterized by link activities, i.e., a pattern of node-node communications on who is communicating with whom and when. For wireless networks, both a physical and a logical configuration can vary due to either failures or environmental changes. Configuration management is to adapt a physical and/or a logical topology to support and maintain node-node communications.

There is no centralized management authority for infrastructureless wireless networks. Self-configuration is desirable for nodes to adjust adaptively their own positions and communication activities in a distributed setting through local interactions. A challenge is whether distributed self-configuration would result in a near-optimal configuration with a sufficiently small approximation error.

In this work, we develop an analytical model for distributed self-configuration, and study the issue of near-optimality. To be specific, we consider joint formation and re-configuration of a physical topology and scheduling upon node failures. For simplicity, we focus on ad-hoc wireless networks with node failures and random perturbations of positions but without mobility. Our prior work [13] developed an initial probabilistic graphical model for the distributed configuration. This work enhances modeling, analysis on the performance-complexity trade-off, and validation through simulation.

What is optimality? Deterministic optimization has been used to obtain an optimal solution for centralized management [2][3][4][23]. A cost function is derived to consist of management objectives and constraints. Such an approach has been applied to network capacity maximization through adapting a physical topology [8], and to link-scheduling through configuring a logical topology [2]. Open issues are how to include random factors such as inaccurate node positions, wireless channels, interference, and locally interacting wireless nodes. Another open issue is whether a cost function itself is optimal, which may go beyond a conventional optimization framework.

From a computational standpoint, global optimization requires a centralized entity to maintain and update complete information for all nodes in the network. This is impractical for large networks. More importantly, locality can be a generic feature to configuration management. For example, in a large wireless network, nodes and links often fail locally. A local repair is thus desirable for preventing an entire network from an incessant re-configuration. Therefore, distributed configuration management is a necessity for large wireless networks [2][13].

In a distributed setting, each node either adjusts its own physical position or decides when and whom to transmit based on local information. This should be done in a fully

S. Jeon and C. Ji are with the School of Electrical and Computer Engineering, Georgia Institute of Technology, Atlanta, GA 30332 USA. E-mail: sujeon@microsoft.com and jic@ece.gatech.edu

asynchronous and distributed fashion with local information exchange. Local information on a configuration may include physical locations and communication activities (channel-access) of neighbors. Such information can be either sensed locally at a node or exchanged with neighbors. The range of information-exchange characterizes communication complexity. When the information-exchange is performed only among close neighbors, the resulting distributed algorithm would scale gracefully with a network size.

Numerous distributed algorithms and protocols have been developed for topology formation [28][30] using local information (see [33] and references therein). Self-organizing protocols have been developed for sensor networks [5][26] and p2p self-stabilizing networks (see [18] and references therein). These distributed algorithms are deterministic. [25] uses a simple randomized algorithm to analyze throughput for different traffic conditions of wireless ad-hoc networks. [29] develops a fast randomized and distributed algorithm for edge coloring, assuming a bounded nodal degree on bipartite graphs and thus Markovian dependence. [1] develops a probabilistic model with spatial Markovian assumptions to characterize the randomness in node positions. [24] uses gossiping algorithms to show that the throughput of wireless networks can be maximized in a fully distributed fashion. These randomized algorithms either assume Markovian spatial dependence which results in the optimality or require non-local information for local-decisions. [4] [23] show that more general SINR-based interference models result in non-Markovian (long-range) spatial dependence, and the aggregated interference from small interfering links of different strengths may not be negligible [4]. [16] proposes a measurement-based self-organization for 802.11 wireless access network. [16] is based on a Gibbs distribution, thus the global optimality can be achieved asymptotically as shown in [7]. However, different from 802.11 wireless access networks, nodes in ad hoc wireless networks may not have complete information especially from far-away nodes.

A question arises [24], if the spatial dependence is non-Markovian, when is distributed configuration management near optimal? Thus, quantitative conditions need to be derived on *when* and *how* the distributed management can result in a near-optimal configuration. In fact, it has been considered as a difficult problem in general to develop a distributed algorithm with a predictable performance [31]. The open questions are

- *What* measures the optimality of centralized-configuration management, and the near-optimality of distributed-configuration management?
- *When* is it possible for distributed management to achieve a near-optimal configuration?
- *How* to derive distributed algorithms that obtain a near-optimal configuration?

This work intends to develop a framework to study these issues through *modeling*, *analysis*, and *algorithms*.

Global Model and Optimality: The optimality of configuration management can be considered in a model-based framework. There, if network configurations can be modeled based on the ground truth, the optimality can be defined accordingly. Centralized configuration management can be used to define the optimality of a network configuration as nodes are not limited by the scope of information exchange.

We consider three factors in a model of configuration: Randomness resulting from a network internally, management constraints imposed externally, and distributed decisions made by nodes with limited information. Randomness in wireless networks is challenging to model [13]. This work begins with simple scenarios where the randomness results from perturbed node positions, interference, and node-node communication. Fading is not considered in this work for simplicity. Management constraints include requirements on the connectivity of a physical topology, signal-to-interference plus noise ratio (SINR) and reconfiguration cost. Nodes make asynchronous and randomized decisions, adjusting a configuration in a distributed setting. The model is developed from bottom-up by mapping these three factors onto a probability distribution. The model is thus accurate in regard to the "ground truth" based on the assumed wireless channel, constraints and nodal decisions. Overall, such a model characterizes statistical spatial dependence of nodes/links in a network configuration.

To obtain an analytical form of the probabilistic model, we adopt an analogy between link activities and node positions of a wireless network and interacting particles in statistical physics [12][32]. Such an analogy allows the use of "configuration Hamiltonian" [19] for quantifying a network configuration. The configuration Hamiltonian corresponds to an artificial system energy of a wireless network. The system energy combines the physical topology, link activities, and management constraints into a single quantity. The configuration Hamiltonian is then used to obtain a probabilistic model which is known as a Gibbs distribution [12]. Such a Gibbs distribution is for an entire "network" configuration and thus corresponds to a global probabilistic model.

Local Model and Probabilistic Graphs: We obtain a local model as an approximation of the global model of network configurations. To approximate the global model, we rely on a one-to-one mapping between a Gibbs distribution and a probabilistic graphical model in machine learning [7][15]. The graph provides a simple and explicit representation of statistical spatial dependence in a network configuration.

We show that a probabilistic graph of the global model belongs to a two-layer random-field. One layer is for a physical configuration, and the other layer is for a logical configuration. The graph is fully connected , i.e., non-Markovian, where the long-range spatial dependence results from the interference among far-away nodes. When the long-range interference can be neglected, the global model can be approximated by a two-layer coupled Markov Random Field which is also called a Random Bond model. The corresponding dependency graph exhibits a nested spatial Markov dependence for both a physical and logical configuration. Mathematically, such a spatial Markov dependence can be represented as a product of local conditional probability density functions [7]. Hence the probabilistic graphical model shows which "dependency links" to remove, result in a local model.

We define an approximation error to measure the difference between the local and global model. When the approximation error is within a given bound, a local model is near-optimal. We then define complexity to characterize the size of a neighborhood where nodes exchange information locally. We obtain bounds for the approximation error. The approximation error and the bounds depend on the following parameters from the physical and logical configuration: the power decay of a wireless channel, the density of active (transmitting) nodes, the complexity, and the size of a network. We quantify the impact of these interacting parameters on the approximation error for a large network. We derive sufficient conditions for the local model to be near-optimal, i.e., when the total interference from far-away nodes decreases faster than the growth of the number of interfering nodes as the network size increases.

Distributed Algorithm: A local model results in a class of distributed algorithms where nodes self-configure through information exchange with neighbors. The range of information exchange characterizes the local connectivity of the probabilistic dependency graph, and corresponds to the communication complexity. The actual information exchanged includes relative positions of neighbors and activities of adjacent nodes. Node decisions are probabilistic, corresponding to randomized distributed algorithms of graphical models.

We apply the distributed algorithm to three examples of self-configuration: (a) forming a 1-connected physical topology from a random initial topology; (b) configuring a logical topology that maximizes spatial channel-reuse and incessant communication demands; and (c) reconfiguring jointly a physical- and logical-configuration upon failures. We use simulation to validate the models and bounds, and demonstrate how the framework enables fully distributed spatial scheduling algorithms and fault tolerance for wireless infrastructureless networks.

II. Problem Formulation

A. Assumptions

Consider a wireless network with the following assumptions.

Physical Layer: All nodes share a common frequency channel. A pair of nodes within a communication range can communicate directly with an omni-directional antenna. The wireless channel follows a path-loss model with a power attenuation of factor $\alpha \in \{2 \sim 6\}$. Shadowing and/or multi-path fading are not considered in this work for simplicity. Node i transmits with power P_i, where $0 \leq P_i \leq P_{max}$, $1 \leq i \leq N$, with P_{max} being the maximum transmission power, and N being the number of nodes in the network. Power control is not considered in this work.

MAC Layer: Let SINR_{th} be a given threshold for the SINR requirement. Node i can transmit to node j when the SINR requirement is satisfied, i.e., $\text{SINR}_{ij} = \frac{P_i l_{ij}^{-\alpha}}{N_b + \sum_{(m,n)\neq(i,j)} P_m l_{mj}^{-\alpha}} \geq \text{SINR}_{th}$, where l_{ij} is the distance between nodes i and j, and N_b is the noise power. We consider a scheduled resource allocation that is implemented with local interactions among neighbors.

Configuration Management: Let X_{i0} and X_i be a desired and an actual location of node i, for $1 \leq i \leq N$. $\boldsymbol{X} = \{X_1, \cdots, X_N\}$ are random positions of nodes in a network where the randomness results from perturbed positions, random movements and measurement errors.

Let σ_{ij} denote channel-access of link (i,j), where $\sigma_{ij} = 1$ if node i is transmitting to node j; and $\sigma_{ij} = -1$, otherwise. σ_{ij} is referred to as a "communication dipole" in this work, for $1 \leq i,j \leq N$, $i \neq j$, and $\boldsymbol{\sigma} = \{\sigma_{1,2}, \cdots, \sigma_{N,N-1}\}$ denotes a set of link activities in the network. Link activities are assumed to be random as they are triggered by network-layer random traffic demands. A logical configuration is $\boldsymbol{\sigma} = \{\sigma_{ij}\}$. A network configuration is $(\boldsymbol{\sigma}, \boldsymbol{X})$.

The objectives are to achieve distributed configuration management, i.e., to (a) form a desired physical topology, (b) schedule the resource utilization at a given time to maximize the spatial channel-reuse with a desired SINR requirement, and (c) reconfigure upon failures by minimizing reconfiguration cost.

B. Formulation

Let $\text{P}(\boldsymbol{\sigma}, \boldsymbol{X})$ be a true probabilistic global model of a network configuration that results from the above assumptions.

Definition 1: *Optimal Configuration. $(\boldsymbol{\sigma}^*, \boldsymbol{X}^*)$ is an optimal configuration if it maximizes the global likelihood,*

$$(\boldsymbol{\sigma}^*, \boldsymbol{X}^*) = arg \max_{(\boldsymbol{\sigma}, \boldsymbol{X})} P(\boldsymbol{\sigma}, \boldsymbol{X}). \quad (1)$$

Let $P^l(\boldsymbol{\sigma}, \boldsymbol{X})$ be a local model that approximates the global model $\text{P}(\boldsymbol{\sigma})$.

Definition 2: *Near-Optimal Configuration. Consider $(\hat{\boldsymbol{\sigma}}, \hat{\boldsymbol{X}})$ that maximizes $P^l(\boldsymbol{\sigma}, \boldsymbol{X})$, i.e.,*

$$(\hat{\boldsymbol{\sigma}}, \hat{\boldsymbol{X}}) = arg \max_{(\boldsymbol{\sigma}, \boldsymbol{X})} P^l(\boldsymbol{\sigma}, \boldsymbol{X}). \quad (2)$$

Consider an approximation error as the average relative difference between the log likelihoods,

$$E[\Delta] = E\left[\left|\frac{\log P(\boldsymbol{\sigma}^*, \boldsymbol{X}^*) - \log P(\hat{\boldsymbol{\sigma}}, \hat{\boldsymbol{X}})}{\log P(\boldsymbol{\sigma}^*, \boldsymbol{X}^*)}\right|\right], \quad (3)$$

where the expectation is over $\hat{X}$, X^*, σ^*, and $\hat{\sigma}$. For a given $\epsilon > 0$, if $E[\Delta] \leq \epsilon$, the local model $P^l(\boldsymbol{\sigma}, \boldsymbol{X})$ and the corresponding realization $(\hat{\boldsymbol{\sigma}}, \hat{\boldsymbol{X}})$ are near-optimal.

Distributed configuration management requires that $P^l(\boldsymbol{\sigma}, \boldsymbol{X})$ is factorizable, i.e., $P^l(\boldsymbol{\sigma}, \boldsymbol{X}) = \prod_{ij} g_{ij}(\boldsymbol{\sigma}, \boldsymbol{X})$, where $g_{ij}(\boldsymbol{\sigma}, \boldsymbol{X})$ is a localized probability density function that depends on variables in a neighborhood of nodes i, j and link (i,j) for $1 \leq i,j \leq N$. The global maximization from Eq.(1) reduces to a set of coupled local maximizations, i.e., $(\hat{\sigma}_{ij}, \hat{X}_i) = \arg\max_{(\sigma_{ij}, X_i)} g_{ij}(\boldsymbol{\sigma}, \boldsymbol{X})$ for $1 \leq i,j \leq N$.

Note that when variables exhibit spatial Markovian dependence, distributed configuration management is naturally

optimal[7]. But when variables are non-Markovian, the near-optimality becomes important. Hence, $E[\Delta]$ provides a performance bound of distributed configuration management. If $E[\Delta]$ is less than a given error, the near-optimality can be achieved by a fully distributed configuration management based on co-operations of nodes in a small neighborhood.

Our tasks are to

(a) obtain a global model P($\boldsymbol{\sigma}, \boldsymbol{X}$) from the above given assumptions;

(b) characterize the spatial dependence of multiple variables ($\boldsymbol{\sigma}, \boldsymbol{X}$) using a graphical representation of P($\boldsymbol{\sigma}, \boldsymbol{X}$). Obtain a simplified graph and a mathematical representation for $P^l(\boldsymbol{\sigma},\boldsymbol{X})$;

(c) obtain sufficient conditions for $P^l(\boldsymbol{\sigma},\boldsymbol{X})$ to result in a near-optimal configuration;

(d) derive a distribution algorithm, and apply the algorithm to self-configuration.

Table I summarizes key notations used in the paper.

TABLE I
IMPORTANT NOTATIONS

α	Power attenuation factor, $2 \leq \alpha \leq 6$
N_b	Power of channel noise
SINR$_{ij}$	$\frac{P_i l_{ij}^{-\alpha}}{N_b+\sum_{(m,n)\neq(i,j)} P_m l_{mj}^{-\alpha}}$
σ_{ij}	Activity of link (i,j), $\sigma_{ij} \in \{-1,1\}$, $\eta_{ij}=\frac{\sigma_{ij}+1}{2}$
X_i	Position of node i
$E(\Delta)$	Approximation error of the local model
ϵ_Δ	An upper-bound of approximation error $E(\Delta)$
ϵ	Desired threshold of approximation error $E(\Delta)$
Z	Normalization constant

III. GLOBAL MODEL

We begin by developing a global model that characterizes probabilistic spatial dependence in a network configuration. Our approach is bottom-up so that the probabilistic model can be obtained faithfully based on the given assumptions and management constraints.

A. Logical Configuration

We begin with modeling a logical configuration given node positions. A logical configuration is considered as random, detailed explanations and an example can be found in [14].

1) Configuration Hamiltonian: We now develop a probabilistic model for logical configuration $\boldsymbol{\sigma}$ given a set of node positions $\boldsymbol{X}$. We regard $\boldsymbol{\sigma}$ as a set of communication dipoles. Terminology "dipole" is originally used in a particle system in statistical physics. There, a dipole corresponds to a particle with binary states, active or inactive [19]. Now consider each "communication dipole" as a particle. Table I compares a wireless network with a particle system through their similarities.

TABLE II
CORRESPONDENCE BETWEEN WIRELESS (DIPOLE) NETWORK AND PARTICLE SYSTEMS

Wireless (Dipole) Network	Particle Systems (Lattice Gas [19])
active(+1) / inactive(-1)	occupied(+1) / empty(-1)
interference	interaction energy
system potential energy	chemical potential
logical configuration	system state (e.g., liquid or gas)

Configuration Hamiltonian has been applied to a particle system to describe the states of a set of particles under the following conditions: (a) active particles are statistically distinguishable, and (b) interactions between particles are weak.

We now extend the notion of configuration Hamiltonian to the wireless network, where active communication dipoles are statistically distinguishable; and interactions among dipoles are weak due to decaying interference. We define a system energy of a logical configuration as the summation of the received power at individual receivers in the network,

$$\sum_{ij} P_j \cdot \frac{\sigma_{ij}+1}{2}, \tag{4}$$

where P_j denotes the net received-power at the receiver j by considering the signal component, interferences and noise. Note that for a link (i,j) where node i is a transmitter and j is a receiver, P_i denotes the transmission power of transmitter i, and P_j denotes the received power at receiver j. We define the received power P_j to include the transmitted signal from the transmitter i and the interference from interferers with the opposite sign of the signal from transmitter i. Based on the assumptions in Section II, for a single active dipole $\sigma_{ij} = 1$ in the network, the received power at the receiver $P_j = P_i l_{ij}^{-\alpha} \frac{\sigma_{ij}+1}{2}$, where $l_{ij} = |X_i - X_j|$. A dipole is inactive, i.e., $\sigma_{ij} = -1$ and $P_j = 0$, if node i does not transmit to node j. For multiple active dipoles, P_j has addition terms as the interference.

Following the definitions in statistical physics [12], the "configuration Hamiltonian" of a dipole system is the negative system energy [13],

$$H(\boldsymbol{\sigma}|\boldsymbol{X}) = -\sum_{ij} P_j \eta_{ij} + \beta \sum_{ij} (\text{SINR}_{ij} - \text{SINR}_{th})^2 \eta_{ij}, \tag{5}$$

where $\eta_{ij} = \frac{\sigma_{ij}+1}{2}$, $\text{SINR}_{ij} = \frac{P_i l_{ij}^{-\alpha} \eta_{ij}}{\sum_{mn\neq ij} P_m l_{mj}^{-\alpha} \eta_{mn} + N_b}$ is the SINR for dipole σ_{ij}, SINR_{th} is a given SINR threshold, and $\beta > 0$ is a weighting factor. $\beta(\text{SINR}_{ij} - \text{SINR}_{th})^2$ serves as a penalty term for the SINR constraint[1], an equivalence of which is used for simplicity, i.e., $\beta[P_i l_{ij}^{-\alpha} \eta_{ij} - \text{SINR}_{th}(\sum_{mn\neq ij} P_m l_{mj}^{-\alpha} \eta_{mn} + N_{b_{ij}})]^2$.

For an active dipole $\sigma_{ij} = 1$, the interference sources within a certain neighborhood from the receiver j are considered as

[1]The use of a quadratic function as the constraint is for simplicity of derivation. A hard constraint is used in the distributed algorithm, i.e., $\beta U(\text{SINR}_{th} - \text{SINR}_{ij})$ where $U(x) = 1$ for $x > 0$; 0, otherwise.

the significant interferers; and this neighborhood is denoted by N_{ij}^I as the interference range of node j. The Hamiltonian can be rewritten as

$$H(\boldsymbol{\sigma}|\boldsymbol{X}) = R_1(\boldsymbol{\sigma},\boldsymbol{X}) + R_2(\boldsymbol{\sigma},\boldsymbol{X}) + R_3(\boldsymbol{\sigma},\boldsymbol{X}) + R_I(\boldsymbol{\sigma},\boldsymbol{X}), \quad (6)$$

where $R_1(\boldsymbol{\sigma},\boldsymbol{X}) = \sum_{ij} \alpha_{ij}\eta_{ij}$ is the first-order energy of individual dipoles, $R_2(\boldsymbol{\sigma},\boldsymbol{X}) = \sum_{ij}\sum_{mn \in N_{ij}^I} \alpha_{ij,mn}\eta_{ij}\eta_{mn}$ is the second-order energy with products of two dipoles within the interference range, $R_3(\boldsymbol{\sigma},\boldsymbol{X}) = \sum_{ij}\sum_{mn \in N_{ij}^I} \sum_{uv \in \{N_{ij}^I, N_{mn}^I\}} \alpha_{ij,mn,uv}\eta_{ij}\eta_{mn}\eta_{uv}$ is the third-order energy with products of three dipoles within the interference range, $R_I(\boldsymbol{\sigma},\boldsymbol{X}) = \sum_{ij} R_{I_{ij}}(\boldsymbol{\sigma},\boldsymbol{X})$ is the total interference outside the interference range where $R_{I_{ij}}(\boldsymbol{\sigma},\boldsymbol{X})$ is the residual interference outside the interference range of an active dipole $\sigma_{ij} = 1$. The coefficients of the link activities $\boldsymbol{\sigma}$ depend on relative node positions l_{ij}'s, where

$$\begin{aligned}
\alpha_{ij} &= -P_i l_{ij}^{-\alpha} + \beta \cdot (P_i l_{ij}^{-\alpha} - \text{SINR}_{th} N_b)^2, \quad (7)\\
\alpha_{ij,mn} &= 2\sqrt{P_i P_m} l_{ij}^{-\frac{\alpha}{2}} l_{mj}^{-\frac{\alpha}{2}} - P_m l_{mj}^{-\alpha} + \beta \text{SINR}_{th}^2 P_m^2 l_{mj}^{-2\alpha}\\
&\quad -2\beta(P_i l_{ij}^{-\alpha} - \text{SINR}_{th} N_b) \cdot \text{SINR}_{th} P_m l_{mj}^{-\alpha},\\
\alpha_{ij,mn,uv} &= -2\sqrt{P_m P_u} l_{mj}^{-\frac{\alpha}{2}} l_{uj}^{-\frac{\alpha}{2}} + \beta(\text{SINR}_{th}^2 P_m P_u l_{mj}^{-\alpha} l_{uj}^{-\alpha}).
\end{aligned}$$

Intuitively, α_{ij} corresponds to the increased power when dipole σ_{ij} becomes active, $\alpha_{ij,mn}$ relates to the interference experienced by σ_{ij} resulting from a neighboring active dipole σ_{mn}, and $\alpha_{ij,mn,uv}$ relates to the interference experienced by σ_{ij} from both σ_{mn} and σ_{uv}.

B. Physical Configuration

Now consider node positions $\boldsymbol{X}$. $\boldsymbol{X}$ is assumed to be random where the randomness originates from perturbed node locations, e.g., due to random movements from desired locations and measurement noise. For example, a set of desired positions can be pre-determined as a management constraint to form a regular grid. But the actual node positions may deviate from their desired positions, resulting in an irregular topology.

Management constraints are imposed on the physical connectivity. The 1-connectivity is an example where there exists at least one connected path between any two nodes in the network to achieve the reachability of any source-destination pair. A Yao-graph provides a sufficient condition of the 1-connected physical topology, where each node has a connected link with its nearest neighbors every θ ($\leq \frac{2\pi}{3}$) radian apart [33]. Such a constraint can be represented as

$$h(X_i, X_j) = \begin{cases} 0, & |\frac{l_{ij}-l_{th}}{l_{th}}| \leq \epsilon_0, \\ |l_{ij} - L_{ij}|, & \text{otherwise}, \end{cases} \quad (8)$$

where ϵ_0 is a small positive constant, L_{ij}=$|X_{i0} - X_{j0}|$ is the desired distance [2] of l_{ij}, X_{i0} is a desired position of node i, which can be pre-determined as management objectives, desired positions, or the initial positions to minimize changes in positions, $\forall$ (i,j). The resulting Hamiltonian for the physical topology is

$$H(\boldsymbol{X}) = \sum_i \frac{(X_i - X_{i0})^2}{2\sigma^2} + \zeta \sum_i \sum_{j \in N_i^\theta} h(X_i, X_j), \quad (9)$$

[2]When $L_{ij} = l_{th}$ for a positive constant $l_{th} > 0$, resulting in equally placed nodes and a regular Yao-graph.

where N_i^θ is the set of the nearest neighbors of node i for every θ radian, σ is the variance which is assumed to be the same for all nodes for simplicity, and ζ is a positive weighting constant.

C. Network Configuration

We now consider a network configuration which consists of both a physical and a logical configuration.

1) Network Configuration Hamiltonian: Combining the Hamiltonians from the physical and logical configurations results in an overall network-configuration Hamiltonian,

$$H(\boldsymbol{\sigma},\boldsymbol{X}) = H(\boldsymbol{\sigma}|\boldsymbol{X}) + H(\boldsymbol{X}). \quad (10)$$

2) Gibbs Distribution: A configuration Hamiltonian can be related to a probabilistic model through a Gibbs distribution [19]. Specifically, in a particle system [12], the effective system potential energy $H(\omega)$, known as the configuration Hamiltonian, obeys the Gibbs (or Boltzmann) distribution [12], $P(\omega) = Z_0^{-1} \cdot \exp\left(\frac{-H(\omega)}{T}\right)$, where ω is a multi-dimensional configuration-variable, Z_0 is a normalizing constant and T is the temperature of the particle system [7][12].

Model of logical configuration: For a logical configuration $\boldsymbol{\sigma}$ given node positions $\boldsymbol{X}$, a Gibbs distribution $P(\boldsymbol{\sigma}|\boldsymbol{X})$ can be obtained using configuration Hamiltonian $H(\boldsymbol{\sigma}|\boldsymbol{X})$,

$$P(\boldsymbol{\sigma}|\boldsymbol{X}) = Z_\sigma^{-1} \cdot \exp\left(\frac{-H(\boldsymbol{\sigma}|\boldsymbol{X})}{T}\right), \quad (11)$$

where $Z_\sigma = \sum_{\boldsymbol{\sigma}} \exp\left(\frac{-H(\boldsymbol{\sigma}|\boldsymbol{X})}{T}\right)$ is a normalizing constant and also called the partition function [7]. $T > 0$ is the temperature in statistical physics that characterizes the stability of the system [1][7]. The lower the temperature, the more stable the configuration is. T is used in [7] as a computational variable to obtain the most probable configuration (see Section VI for details).

Model of physical configuration: Similarly, the Gibbs distribution of node positions can be obtained as

$$P(\boldsymbol{X}) = {Z_X}^{-1} \cdot \exp\left(\frac{-H(\boldsymbol{X})}{T}\right), \quad (12)$$

where Z_X=$\sum_{\boldsymbol{X}} \exp\left(\frac{-H(\boldsymbol{X})}{T}\right)$ is a normalizing constant.

Two-layer network model: The Gibbs distribution of an entire network configuration can be obtained using the overall configuration Hamiltonian, which is

$$P(\boldsymbol{\sigma},\boldsymbol{X}) = {Z_0}^{-1} \cdot \exp\left(\frac{-H(\boldsymbol{\sigma},\boldsymbol{X})}{T}\right), \quad (13)$$

where Z_0=$\sum_{(\boldsymbol{\sigma},\boldsymbol{X})} \exp\left(\frac{-H(\boldsymbol{\sigma},\boldsymbol{X})}{T}\right)$ is a normalizing constant.

3) Minimum Hamiltonian and Optimal Configuration: An optimal configuration maximizes the likelihood function,

$$(\boldsymbol{\sigma}^*, \boldsymbol{X}^*) = \arg\max_{(\boldsymbol{\sigma},\boldsymbol{X})} P(\boldsymbol{\sigma}, \boldsymbol{X}) = \arg\min_{(\boldsymbol{\sigma},\boldsymbol{X})} H(\boldsymbol{\sigma}, \boldsymbol{X}), \quad (14)$$

where $H(\boldsymbol{\sigma}, \boldsymbol{X}) = -\log\left[P(\boldsymbol{\sigma}, \boldsymbol{X})\right]/T - \log(Z_0)$. Note the system energy $H(\boldsymbol{\sigma}, \boldsymbol{X})$ incorporates both the randomness and the external management requirements. When the constraints are satisfied, the penalty terms should be diminishing. Therefore, an optimal configuration should satisfy the management objectives of spatial reuse and the constraints.

IV. Local Model

We now seek a local model $P^l(\boldsymbol{\sigma}, \boldsymbol{X})$ that is factorizable as a product of localized probability density functions, and also a good approximation to the global model $P(\boldsymbol{\sigma}, \boldsymbol{X})$. We resort to probabilistic graphical models.

A. Graphical Representation

Probabilistic graphical models relate a probability distribution with a dependency graph of the corresponding random variables [7][15][17]. A node in the graph represents a random variable and a link between two nodes characterizes their statistical dependence. In particular, a set of random variables $\boldsymbol{v}$ forms Gibbs Random Field (GRF) if it obeys a Gibbs distribution [19]. Hammersley-Clifford theorem shows an equivalence between a probabilistic dependency graph and a Gibbs distribution.

Hammersley-Clifford Theorem [19]: *Let $S = \{1, \cdots, N\}$ be a set of nodes, and $\boldsymbol{v}$ be a set of random variables $\boldsymbol{v} = \{v_1, \cdots, v_N\}$. $\boldsymbol{v}$ is said to be a Markov Random Field if (i) P($\boldsymbol{v}$) > 0 for $\forall$ $\boldsymbol{v}$ in sample space; (ii) $P(v_i|\boldsymbol{v_j}$ for $j \in S\backslash\{i\}) = P(v_i|\boldsymbol{v_j}$ for $j \in N_i)$, where N_i is a set of neighbors of node i for $1 \le i \le N$.*

Random field $\boldsymbol{v}$ is also a Gibbs Random Field if its probability distribution can be written in a product form P($\boldsymbol{v}$) = $\prod_{c\in C} V_c(\boldsymbol{v})$, where c is a clique, $\mathcal{C}$ is the set of all feasible cliques, and $V_c(\boldsymbol{v})$ is a positive function.

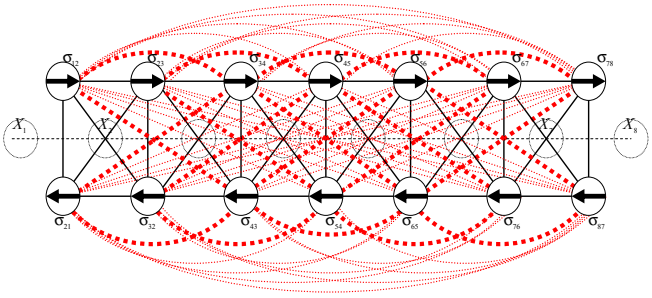

Fig. 1. Dependency Graph of Link Activities $\boldsymbol{\sigma}$ given Node Positions $\boldsymbol{X}$ for a line network. Contention range is given to be one hop and interference range is two hops.

Hammersley-Clifford Theorem asserts that $\boldsymbol{v}$ is a Markov Random Field *if and only if* the probability distribution P($\boldsymbol{v}$) follows a Gibbs distribution with conditional independence given neighbors. This theorem shows an interesting type of probabilistic graphical models where a random variable is conditionally independent of the others given its neighbors. In particular, when the neighborhood is much smaller than the size of a network, the conditional independence implies an interesting type of spatial Markov dependence, i.e., a node depends on its far neighbors through neighbors' neighbors. Such a nested dependence can be shown explicitly through local connectivities among nodes in a dependency graph. The resulting probability distribution is thus factorizable in terms of local probability distributions.

For example, consider a one-dimensional physical topology, and the corresponding dependency graph for link activities $\boldsymbol{\sigma}$ given $\boldsymbol{X}$ shown in Figure 1. Nodes in the graph represent binary random variables σ_{ij}'s, and the links represent their spatial dependence. For example, solid lines show the dependence due to channel contention, the thin dashed lines indicate the dependence due to exact interference, and the thick dashed lines correspond to an approximation of the exact spatial dependence. The first and second rows of dipoles show the activity of bidirectional links.

All communication dipoles are fully connected due to interference, and thus exhibit non-Markovian spatial dependence. Such spatial dependence is represented by the Hamiltonian in Eq.(6) that consists of the products of all dipole-pairs. The fully connected dependency graph shows an uninteresting case of a random field where the neighborhood of a node is the entire network. This implies that obtaining an optimal configuration would require each node to exchange information with all the other nodes in the network.

B. Approximation

To our knowledge, little has been done in the prior work on how to obtain an approximation of a fully connected dependency graph for near-optimal distributed configuration management. We observe that the interference outside the interference range, $R_I(\boldsymbol{\sigma}, \boldsymbol{X})$, can be relatively small compared to the first three terms of the configuration Hamiltonian in Eq.(6). The third-order term, $R_3(\boldsymbol{\sigma}, \boldsymbol{X})$, can be small also compared to the second-order term. That is, in Eq.(6), for an active link (i, j), the third terms include $l_{ij}^{-\alpha/2} l_{mj}^{-\alpha/2} l_{uj}^{-\alpha/2}$ where $l_{mj} >> l_{ij}$ and $l_{uj} >> l_{ij}$; whereas, the second term is only the product of $l_{ij}^{-\alpha/2} l_{mj}^{-\alpha/2}$. Hence, if we use the first two terms to approximate the configuration Hamiltonian, we have

$$H^l(\boldsymbol{\sigma}|\boldsymbol{X}) = \sum_{ij} \alpha_{ij}(\boldsymbol{X})\eta_{ij} + \sum_{ij}\sum_{mn\in N_{ij}^I} \alpha_{ij,mn}(\boldsymbol{X})\eta_{ij}\eta_{mn}, \quad (15)$$

and the corresponding Gibbs distribution is

$$P^l(\boldsymbol{\sigma}|\boldsymbol{X}) = Z_l^{-1} \cdot \exp\left(\frac{-H^l(\boldsymbol{\sigma}|\boldsymbol{X})}{T}\right), \quad (16)$$

where Z_l is a normalization constant.

As the sum in Eq.(15) only involves neighboring dipoles which are within the interference range, the resulting dependency

graph now has a small neighborhood (see the thick dashed-lines in Figure 1). In fact this approximated Markov Random Field is the well-known second-order Ising model [19] where the Hamiltonian $H^l(\boldsymbol{\sigma}|\boldsymbol{X})$ consists of both the first- and second-order terms of σ_{ij}'s. Such an approximation can also be obtained directly from the probabilistic dependency graph of the global model. That is, by removing all edges outside the interference range of each node, we can obtain the graphical representation of the local model.

C. Spatial Dependence in Physical Topology

We now examine the spatial dependence of node positions $\boldsymbol{X}$. In general, spatial dependence in physical topology is not always Markovian since a general management objective can correspond to a fully connected graph. However, for many important and practical management objectives, a node only needs to interact with the close neighbors. Thus we also consider a physical topology that exhibits the second-order Markov dependence in this work.

For example, under the 1-connectivity constraint shown in Eq.(8), node positions $\boldsymbol{X}$ correspond to a second-order Markov Random Field, where the interactions are only with the first-order neighbors.

D. Two-layer Markov Random Fields

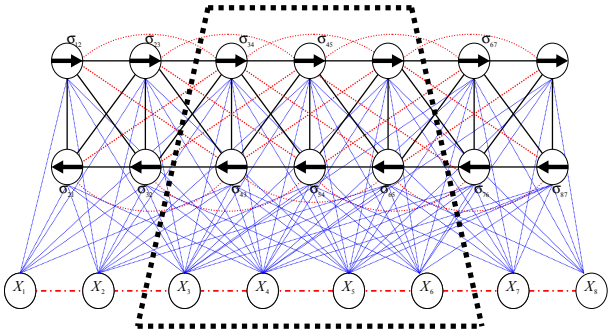

Fig. 2. Two-layer Graph and Clique of ($\boldsymbol{\sigma}$, $\boldsymbol{X}$). The Dashed-Line Box: A Clique of the Two-layer Graph

The probabilistic graph of an overall configuration can be obtained by combining two graphs for the logical and physical configuration. For the example network, a two-layer graph is shown in Figure 2 as an approximation of the original overall configuration. The upper layer graph is for the logical configuration that assumes the local interference among neighboring active dipoles. The lower-layer is for the physical configuration that shows Markov dependence of node positions due to the 1-connectivity constraint in Eq.(8). The entire graph thus exhibits spatial Markov dependence at both layers.

This two-layer graph corresponds to a coupled MRF [7], where an Ising model and a second-order MRF are combined together. The graph is also known as a Random-Bond model [19], where dipoles are connected by random bonds which depend on node positions. The two-layer MRF ($\boldsymbol{\sigma}$, $\boldsymbol{X}$) can also be represented by a chain graph [21] of two MRF layers, one for $\boldsymbol{X}$ and the other for $\boldsymbol{\sigma}$. The two-layer probabilistic graph thus maps the complex spatial dependence of a multi-hop wireless network to an explicit graphical representation.

The corresponding likelihood function can then be represented as

$$P^l(\boldsymbol{\sigma}, \boldsymbol{X}) \propto \prod_{i,j} g_{ij}(\boldsymbol{\sigma}, \boldsymbol{X}), \tag{17}$$

where $g_{ij}(\boldsymbol{\sigma}, \boldsymbol{X})$ is a local probability density function and can be represented as a function of the sum of clique potentials:

$$\begin{aligned} g_{ij}(\boldsymbol{\sigma}, \boldsymbol{X}) &= \prod_{c \in C_{ij}} \exp\left(\frac{-\psi_c(\boldsymbol{\sigma}, \boldsymbol{X})}{T}\right) \\ &= \exp\left(\frac{-\sum_{c \in C_{ij}} \psi_c(\boldsymbol{\sigma}, \boldsymbol{X})}{T}\right), \end{aligned}$$

where C_{ij} is the set of all cliques including node i, node j, and link (i, j); and $\psi_c(\boldsymbol{\sigma}, \boldsymbol{X})$ is a clique potential function of a clique c.

As an example, consider a clique for nodes 3 and 4 as well as link $(3, 4)$ shown in Figure 2. The corresponding potential is a collection of related clique functions, i.e.,
$\sum_{c \in C_{34}} \psi_c(\boldsymbol{\sigma}, \boldsymbol{X}) = \left[\frac{(X_3 - X_3(0))^2}{2\sigma^2} + \zeta \sum_{j \in \{2,4\}} h(X_3, X_j)\right]$ + $\left[\frac{(X_4 - X_4(0))^2}{2\sigma^2} + \zeta \sum_{j \in \{3,5\}} h(X_4, X_j)\right]$ + α_{34} + $\sum_{mn \in \sigma_{N_{34}^I}} (\alpha_{34,mn} + \alpha_{mn,34}) \frac{\sigma_{mn}+1}{2}$, where $\sigma_{N_{34}^I} = \{\sigma_{12}, \sigma_{21}, \sigma_{23}, \sigma_{32}, \sigma_{43}, \sigma_{45}, \sigma_{54}, \sigma_{56}, \sigma_{65}\}$ corresponds to the set of neighboring dipoles of σ_{34} within the interference range. The solid line connecting σ_{34} and σ_{45} indicates the spatial dependence due to the channel contention. The dash line connecting σ_{34} with either X_5 or X_6 indicates the dependence of dipole σ_{34} with positions (X_5,X_6) of a neighboring dipole σ_{56}. In general, a clique is determined by the interference range.

V. Analysis: Near-Optimality and Complexity

We now derive near-optimality conditions for a local model to be a good approximation of the global model. The conditions can be obtained through the approximation error (Eq. (3)), communication complexity, and their trade-offs.

A. Communication Complexity

The neighborhood size in a Markov Random Field corresponds to the range of information exchange of a node with its neighbors, and thus characterizes communication complexity. Specifically, the communication complexity of an active dipole can be regarded as the maximum number of active dipoles within its interference range. As such a maximum number is random and varies from dipoles to dipoles, we use a deterministic bound for the number of active dipoles.

Assume that an active dipole σ_{ij} satisfies the SINR requirement, i.e., $\text{SINR}_{ij} = \frac{P_i l_{ij}^{-\alpha}}{N_b + \sum_{mn \neq ij} P_m l_{mj}^{-\alpha} \frac{\sigma_{mn}+1}{2}} \geq \text{SINR}_{th}$, for $1 \leq, i, j, N$, $i \neq j$. Consider a circle centered at the receiver X_j of the active dipole σ_{ij} within which there cannot exist any active dipoles for the SINR requirement to hold. The radius of the circle is the contention range for node j.

Denote the minimum contention range for all active dipoles as r_c which is the minimum distance between any two active dipoles in the network. Only one dipole can be active within a contention range. Now consider interference range outside the contention range where multiple dipoles can be active concurrently, resulting in interference. We now bound the interference region using a circular region of radius r_f. The region includes active dipoles outside r_c but within r_f shown in Figure 3. Note that the actual interference range of a receiver may not be symmetrical in all directions but bounded by the circular region. This circular region is now considered as the relevant interference neighborhood for node j.

By packing the circular region with small circles of radius r_c, we can obtain the maximum number of active dipoles in the interference neighborhood.

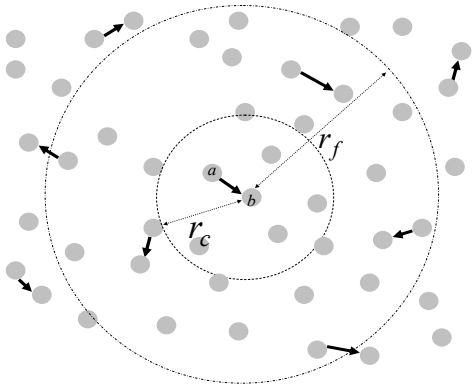

Fig. 3. Contention range r_c and interference range r_f of an active dipole

Definition 3: *Communication Complexity $\mathcal{C}$. The communication complexity of a dipole σ_{ij} is defined as the maximum number of active dipoles within the interference range, i.e., $\mathcal{C} = (\frac{r_f}{r_c})^2$, for $1 \le i, j \le N$, $i \ne j$.*

B. Near-Optimality Conditions

We now derive sufficient conditions for a local model to be a good approximation of the global model. We consider homogeneous networks for ease of analysis.

Theorem 1: *Consider a network where N nodes are uniformly distributed, and satisfies the 1-connectivity where the distance between any node and its neighbors for every θ is between $l_{th}(1-\epsilon_0)$ and $l_{th}(1+\epsilon_0)$, and $0 < l_{th}(1+\epsilon_0) < r_c$. Assume that N nodes transmit at the same power level ($P_t > 0$), have the same desired SINR threshold $SINR_{th}$ and the same circular interference range r_f. Let $\alpha \ge 2$ be the power attenuation factor of the channel. The average approximation error can be bounded as $E[\Delta] \le \epsilon_\Delta$, where*

$$\epsilon_\Delta = \begin{cases} \frac{\mathcal{I}}{r_c^2}\left\{(2+\ln\mathcal{C})^2 + \frac{4\pi}{l_{th}}(r_c + \sqrt{N l_{th} r_c})\right\}, & \alpha = 2 \\ \frac{\mathcal{I}}{r_c^2}\left\{\frac{2(2-\frac{1}{\mathcal{C}})^2}{r_c^2} + \frac{4\pi}{l_{th}^2}(\frac{1}{\sqrt{\mathcal{C}}} + \ln(1+\sqrt{\frac{N l_{th}}{\mathcal{C} r_c}}))\right\}, & \alpha = 4 \\ \frac{\mathcal{I}}{r_c^2}\left\{\frac{2(\alpha-2\mathcal{C}^{\frac{2-\alpha}{2}})^2}{(\alpha-2)^2 r_c^{\alpha-2}} + \frac{4\pi}{l_{th}^{\frac{\alpha}{2}}}\left[\mathcal{C}^{\frac{2-\alpha}{4}} r_c^{\frac{4-\alpha}{2}} + \frac{2}{4-\alpha}\right.\right. & \\ \left.\left.(-(\sqrt{\mathcal{C}} r_c)^{\frac{4-\alpha}{2}} + (\sqrt{\mathcal{C}} r_c + \sqrt{N l_{th} r_c})^{\frac{4-\alpha}{2}})\right]\right\}, & \textit{else;} \end{cases}$$

with $\mathcal{I} = 2 l_{th}^{\frac{\alpha}{2}} / \left(l_{th}^{\frac{-\alpha}{2}} - \sqrt{l_{th}^{-\alpha}/SINR_{th} - N_b/P_t}\right)$.

The proof is given in Appendix I. The above analysis shows that a local model results in two components of the approximation error. "Type-1 error"[3] is due to using a model of a lower order within interference regions, and bounded by the first terms in the above expressions. For a given communication complexity $\mathcal{C}$, the Type-1 error can be made small by choosing a sufficiently large r_c. This would reduce the number of active dipoles as well as the dependence among the active dipoles. "Type-2 error" is due to neglecting the aggregated interference outside the interference range, and upper bounded by the remaining terms in the above expressions. Type-2 error can be made small if the aggregated interference outside the interference range is reduced. Specifically, as shown by the theorem, for $\alpha > 2$ and a given r_c, communication complexity $\mathcal{C}$ needs to grow with respect to network size N for the error to be arbitrarily small. The growth rate depends on the power decay of the channel, since the aggregated interference outside the interference range depends on α. For a slow power decay, i.e., $\alpha = 2$, the above result suggests that the Type-2 error is independent of $\mathcal{C}$, and thus can only be reduced by a sufficiently large r_c.

Channel, contention and network size: Using the upper bound of the approximation error ϵ_Δ, we obtain a sufficient condition on the density of active dipoles for a large network so that the local model is near-optimal.

Corollary 1: *Let ϵ be a desired performance-bound. Assume $N \gg 1$, and $\mathcal{C}$ does not grow with respect to N. We have $\epsilon_\Delta \le \epsilon$ if*

$$r_c \ge \begin{cases} O(N^{\frac{4-\alpha}{4+\alpha}}), & 2 \le \alpha < 4, \\ O(\sqrt{\ln N}), & \alpha = 4, \\ O(1), & \alpha > 4, \end{cases}$$

where $O()$ represents the order for large N.

The proof can be obtained through simple algebraic manipulations from Theorem 1, and is thus omitted[4].

Consider the above expression for large interference where $2 \le \alpha < 4$. This corresponds to such channel environments as

[3]We use the Type-1 and Type 2 errors for convenience and they are different from those in hypothesis testing.

[4]From Theorem 1, $\mathcal{C}$ is a function of r_c; thus, $\mathcal{C}$ is replaced with r_f^2/r_c^2.

free space $\alpha = 2$, obstructed areas in factories $\alpha \in \{2 \sim 3\}$, and urban areas $\alpha \in \{2.7 \sim 3.5\}$. $r_c \geq O(N^{\frac{4-\alpha}{4+\alpha}})$ shows that r_c grows with N sublinearly. If communication complexity $\mathcal{C}$ remains constant when network size N increases, the maximum number of activated dipoles is $o(N^{1-\frac{4-\alpha}{4+\alpha}}) = o(N^{\frac{2\alpha}{4+\alpha}})$, showing a sparsely activated network. Hence, the corresponding Markov Random Field with a small neighborhood size may have insufficiently activated dipoles, and may not be an efficient approximation to the global model[5]

Now consider small interference where $\alpha \geq 4$. This corresponds to such channel environments as shadowed urban areas with $\alpha \in \{4 \sim 5\}$, and obstructed regions in buildings ($\alpha \in \{4 \sim 6\}$) [27]. When $4 < \alpha \leq 6$, $r_c > O(1)$. This implies that r_c can grow with N at an arbitrarily slow rate for the approximation error to be small. The network has densely activated dipoles, i.e., the number of active nodes can be slightly fewer than $O(N)$, showing a densely activated network. This case shows that the Markov Random Field with a small neighborhood now has a sufficient number of activated dipoles, and is thus an efficient approximation to the global model.

Topology: Note that for the uniform network assumed in the theorem, l_{th}, the inter-distance between two neighboring nodes, characterizes the physical topology. Thus, Corollary 1 shows that r_c increases with respect to $l_{th}^{1/3}$ for $2 < \alpha \leq 4$ and l_{th} for $\alpha = 2$. This shows that the rate of growth of the contention range with respect to the inter-node distance.

Performance-complexity trade-off: We now examine how $\mathcal{C}$ can vary with respect to α for large N.

Corollary 2: *Assume $N \gg 1$ (and $\mathcal{C} < N$). ϵ_Δ can be simplified as*

$$\epsilon_\Delta = \begin{cases} \frac{\mathcal{I}}{r_c^2}\left\{(2+\ln \mathcal{C})^2 + \frac{4\pi}{l_{th}}(\sqrt{N l_{th} r_c}) + o()\right\}, & \alpha = 2 \\ A_4 (N l_{th} r_c)^{\frac{4-\alpha}{4}} + o(), & 2 < \alpha < 4 \\ \frac{\mathcal{I}}{r_c^2}\left\{\frac{2(2-\frac{1}{\mathcal{C}})^2}{r_c^2} + \frac{4\pi}{l_{th}^2}(\frac{1}{\sqrt{\mathcal{C}}} + \frac{1}{2}\ln(\frac{N l_{th}}{\mathcal{C} r_c}))\right\}, & \alpha = 4 \\ A_1 + A_2 \frac{1}{\mathcal{C}^{\frac{\alpha-2}{4}}} + A_3 \frac{1}{\mathcal{C}^{\frac{\alpha-4}{4}}} + O(N^{\frac{4-\alpha}{4}}), & \alpha > 4; \end{cases}$$

where $A_1 = \frac{\alpha^2 \mathcal{I}}{r_c^\alpha (\alpha-2)^2}$, $A_2 = \frac{4\pi\mathcal{I}}{(l_{th} r_c)^{\frac{\alpha}{2}}}$, $A_3 = \frac{-2\mathcal{I}}{(4-\alpha) r_c^{\frac{\alpha}{2}}}$, $A_4 = \frac{\mathcal{I}}{r_c^2}$.

The proof can be obtained by rewriting ϵ_Δ and simple algebraic manipulations, and thus omitted. The corollary shows that the larger the communication complexity $\mathcal{C}$, the larger the Type-1 error, since more dependency is neglected by the local model within an inference range. In addition, a larger $\mathcal{C}$ should result in a smaller Type-2 error. However, for $2 \leq \alpha \leq 4$, the bound for the Type-2 error is nearly independent of $\mathcal{C}$ for large network size N. This suggests that the strong interference outside $\mathcal{C}$ dominates for a slow decaying channel, and a Markov Random Field may not efficiently approximate a global model. For $\alpha > 4$, ϵ_Δ monotonically decreases as $\mathcal{C}$ increases, suggesting that the spatial dependence within an interference range dominates for a rapidly decaying channel. In fact, ϵ_Δ can be made arbitrarily small if $\mathcal{C}$ and r_c grow at a slow rate with respect to N. Markov Random Fields are thus an efficient approximation of the global model.

Figure 4 shows an example of ϵ_Δ as a function of $\mathcal{C}$ and α for $\text{SINR}_{th} = 20$, $N_b = 0.1$, $r_c = 10$, $r_f \in \{20 \sim 100\}$, $N = 1000$, and $l_{th} = 2$ $meter$[6]. The flat region in Figure 4 corresponds to small α (large interference), where the SINR requirement is violated and ϵ_Δ is truncated to remain constant for illustration. In contrast, ϵ_Δ is less than 10% for $\alpha = 4$ and below 1% for $\alpha = 6$ as shown in the figure.

Figure 4 shows a trade-off between the approximation error and the communication complexity for $\alpha = 4$. The intersection $\mathcal{C}$ and ϵ_Δ, e.g. between the two thick lines in the figure, corresponds to an optimal neighborhood with $\mathcal{C}$=16. This corresponds to [7] $r_f = 40$ and $r_c = 10$. In general, for a given r_f, r_c can be adjusted to vary $\mathcal{C}$ so that a proper trade-off can be obtained. A wide range of $3 \sim 20$ hops for r_c would be the most feasible scenarios.

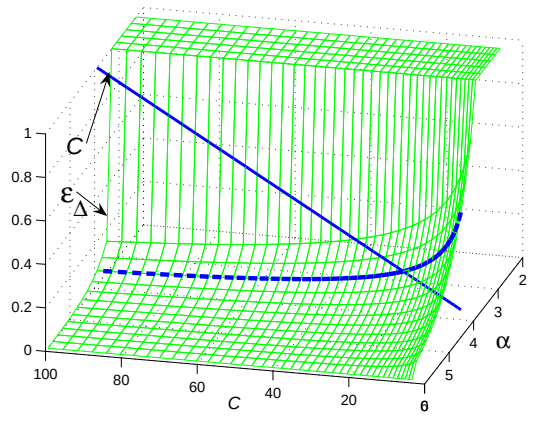

Fig. 4. Trade-off between performance and complexity. Thick dashed line: α=4.

VI. Distributed Algorithm

We now describe randomized distributed algorithms enabled by the local model for self-configuration where nodes make decisions using local information from neighbors.

A. Distributed Algorithm

The distributed algorithm obtains a near-optimal configuration by maximizing the approximated likelihood function,

$$(\hat{\boldsymbol{\sigma}}, \hat{\boldsymbol{X}}) = \arg\max_{(\boldsymbol{\sigma}, \boldsymbol{X})} P^l(\boldsymbol{\sigma}, \boldsymbol{X}). \quad (18)$$

[5] Note that a lower bound would be needed for the approximation error to draw a definitive negative conclusion.

[6] This corresponds to sensor networks for habitat monitoring, battlefield surveillance, and mechanical measurement and monitoring.

[7] In general, an actual optimal value of r_f depends on a constant that weights the relative importance of performance and complexity.

Due to the spatial Markov property, $P^l(\boldsymbol{\sigma}, \boldsymbol{X})$ is factorizable over cliques. Maximizing the likelihood function reduces to maximizing the local probability density functions (clique potentials), i.e., for $1 \leq i, j \leq N$,

$$(\hat{\sigma_{ij}}, \hat{X}_i) = \arg \max_{(\sigma_{ij}, X_i)} P^l(\sigma_{ij}, X_i | X_{N_i}, \sigma_{N_{ij}}), \qquad (19)$$

where $P^l(\sigma_{ij}, X_i | X_{N_i}, \sigma_{N_{ij}}) = g_{ij}(\boldsymbol{\sigma}, \boldsymbol{X})$, X_{N_i} and $\sigma_{N_{ij}^I}$ are in the neighborhood of node i and dipole σ_{ij}, respectively. These local probability density functions are composed of the neighboring nodes and dipoles, and the configuration can thus be updated locally. The local maximizations result in coupled equations due to the nested Markov dependence among random variables of $\boldsymbol{\sigma}$ and $\boldsymbol{X}$, showing the need of information exchange among neighbors.

Many algorithms can be used to maximize the local probability density functions, e.g., stochastic relaxation [7][1] and message passing [17]. This work uses stochastic relaxation which is a randomized algorithm. The algorithm converges to the global maximum of $P^l(\boldsymbol{\sigma}, \boldsymbol{X})$ asymptotically with probability one [7].

In stochastic relaxation, each node makes local decisions based on a certain probability. That is, node i decides X_i and $\{\sigma_{ij}\}$ for $j \in N_i$, which results in a joint optimization of the topology and scheduling. Specifically, let $\hat{X}_i(t+1)$ and $\hat{\sigma}_{ij}(t+1)$ denote the new position that node i would move to and the activity of link (i, j) at time $t+1$, respectively. A sequential implementation of the distributed stochastic algorithm at a node i is described as follows: for $t \geq 1$ and $1 \leq i \leq N$,

(a) given neighbor positions X_{N_i} in the neighborhood N_i of node i, determine $\hat{X}_i(t+1) = x_i$, with probability $P^l\left(X_i(t+1) = x_i | X_{N_i}(t)\right) = \frac{\exp(-\psi_i(x_i)/T(t+1))}{\sum_{\forall x_i} \exp(-\psi_i(x_i)/T(t+1))}$, where $\psi_i(x_i) = \frac{(x_i - X_{i0})^2}{2\sigma^2} + \zeta \sum_{j \in N_i^\theta} h(x_i, X_j(t))$.

(b) Given link activities $\sigma_{N_{ij}}$ and positions X_{N_i} of nodes in the neighborhood of node i, determine whether node i transmits to node j for $\forall j \in N_i$, i.e., $\hat{\sigma}_{ij}(t+1) = \sigma_{ij}$ with probability $P^l\left(\sigma_{ij}(t+1) = \sigma_{ij} | X_{N_i}(t), \sigma_{N_{ij}}(t)\right) = \frac{\exp(-\psi_{ij}(\sigma_{ij})/T(t+1))}{\sum_{\forall \sigma_{ij}} \exp(-\psi_{ij}(\sigma_{ij})/T(t+1))}$, where $\psi_{ij}(\sigma_{ij}) = (\alpha_{ij} + \sum_{mn \in N_{ij}^I} [\alpha_{ij,mn} + \alpha_{mn,ij}] \frac{\sigma_{mn}(t)+1}{2}) \frac{\sigma_{ij}+1}{2}$.

Temperature T is used as a cooling constant in the algorithm, where $T(t) = T_0/\log(1+t)$ varies with time t and T_0=3 [1][19]. This allows an almost-sure convergence to the global minimum of the Hamiltonian (see [7] for more details).

Note that the joint configuration results directly from the distributed algorithm, i.e., given $\sigma_{N_{ij}}$ and positions X_{N_i}, $(\hat{X}_i(t+1), \hat{\sigma}_{ij}(t+1)) = (x_i, \sigma_{ij})$ with probability $P^l\left((X_i(t+1), \sigma_{ij}(t+1)) = (x_i, \sigma_{ij}) | X_{N_i}(t), \sigma_{N_{ij}}(t)\right)$.

B. Information Exchange

At time t, each node (e.g. node i) broadcasts its position and adjacent link status, $(X_i(t), \sigma_{ij}(t) = 1)$, to the neighboring active dipoles. At time $t+1$, node i uses the information received from neighbors, i.e., $(X_m(t), \sigma_{mn}(t) = 1)$ for $m \in N_i$, to update its own local configuration, $X_i(t+1)$ and $\{\sigma_{ij}(t+1)\}$. Here $\{\sigma_{ij}(t+1)\}$ denotes the set of adjacent dipoles of node i. Meanwhile, a node that receives a message ($X_i(t)$, $\sigma_{ij}(t)$=1) also relays the message to its neighbors.

Such information exchange bears a similar spirit to that of Bellman-Ford routing algorithm. Hence the near-optimal distributed algorithm uses relative geo-location information and link activities from neighbors. Note that as an implementation issue, neighbor positions can also be sensed at a node to avoid information exchange among neighbors.

VII. Self-Configuration: Example and Validation

We now apply the distributed algorithm to examples of self-configuration of wireless networks for (a) 1-connectivity formation of physical topology; (b) scheduling for a logical configuration; and (c) localized failure adaptation. We also compare the performance of the randomized distributed algorithm with the centralized algorithm from the global model and the commonly-used distributed protocol model[6][9][22].

A. Example of Self-Configuration

We simulate the distributed algorithm for self-configuration using the following parameters: Network size $N = 100$, the threshold of the inter-node distance $l_{th} = 2$ and $\theta = \frac{\pi}{2}$ for the 1-connectivity of the physical topology, $\alpha = 4$ for the channel, and $\text{SINR}_{th} = 20$. Topologies are randomly generated first. Figure 5 (a) shows an example of a random initial configuration ($\boldsymbol{\sigma_0}$=$\mathbf{0}$, $\boldsymbol{X_0}$). Each node then updates its position based on the iterative statistical local rules using information from its neighbors as in Section VI-A. The iteration stops when a steady state is reached[8]. The dots in Figure 5 (b) show a resulting physical topology with 1-connectivity. The physical topology then remains fixed during formation of a logical configuration. A logical configuration is obtained similarly by the probabilistic local rules in Section VI-A given the physical configuration. Figure 5 (b) also illustrates the resulting logical configuration at the first time epoch.

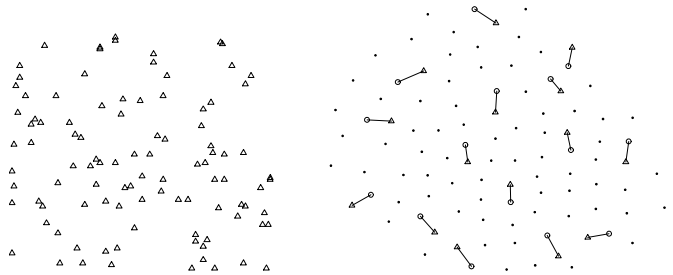

(a) $\boldsymbol{X_0}$ (b) $\boldsymbol{\sigma}$ given $\boldsymbol{X}$

Fig. 5. Self-configuration with localized algorithm

Now, consider that a certain nodes fail in a network configuration shown in Figure 5 (b). Upon failures, the closest

[8]For instance, the condition of $\left|\frac{|X_i - X_j| - l_{th}}{l_{th}}\right| < 0.01$ is satisfied for $\forall i$ and $j \in N_i^\theta$.

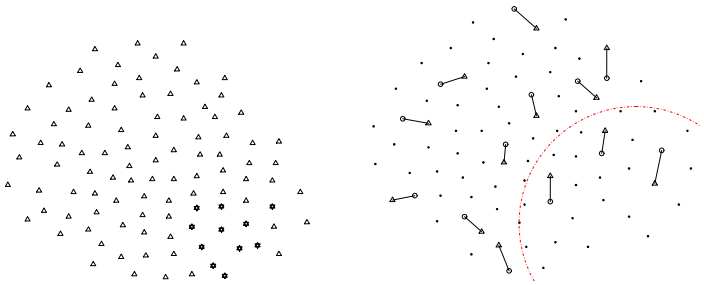

(a) Random failure of nodes (b) Localized recovery of $\boldsymbol{\sigma}$

Fig. 6. Localized recovery from random node failures

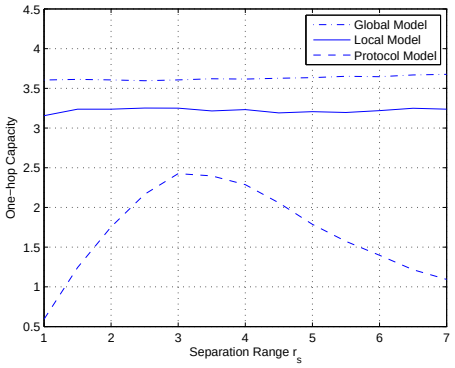

Fig. 8. Comparison of One-hop Capacity: Global, Local, and Protocol Model

neighbors of failed nodes first adjust their positions and select other nodes for transmission. This may cause adjustments to the neighbors and neighbors' neighbors, resulting in cascading changes across the entire network. Hence small perturbations in a network can cause incessant changes to the entire network configuration. Thus localizing failure events is important. Additional penalty terms can be introduced to the Hamiltonian as reconfiguration costs to penalize cascading changes: $\xi \cdot |(\boldsymbol{\sigma}, \boldsymbol{X}) - (\boldsymbol{\sigma}_s, \boldsymbol{X}_s)|$, where $(\boldsymbol{\sigma}_s, \boldsymbol{X}_s)$ denotes the steady-state network configuration, and ξ is a positive weighting constant that characterizes the cost of change in node positions and/or link activities. Such a constraint would localize the change.

Figure 6 (a) shows failures of wireless nodes that are marked as stars. Localized recovery of the physical topology is shown in Figure 6 (b). The nodes outside the arc are not affected by failures; the resulting configuration, however, is no longer globally optimal. The failed logical topology can be locally recovered using the same algorithm also shown in Figure 6 (b).

Figure 7 shows the joint optimization of $\boldsymbol{\sigma}$ and $\boldsymbol{X}$. The joint optimization is done at a node-dipole pair, i.e., $\{X_i, \sigma_{ij}\}$ for $j \in N_i$ first, and then moved on to another node-dipole pair $\{X_m, \sigma_{mn}\}$ for $n \in N_m$, and so on. Compared to the sequential configuration in Figure 5.(b), the joint optimization in Figure 7 increases the number of active dipoles by 30% (from 15 to 20).

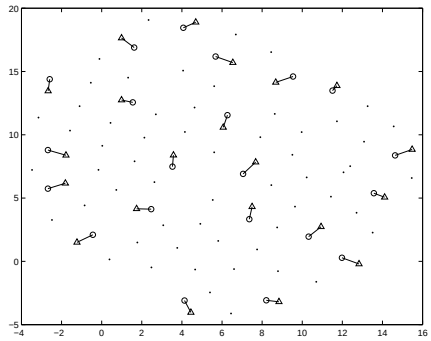

Fig. 7. Joint Optimization of Link Activities and Node Positions

B. Model Validation

We now validate the performance of the local model, communication complexity and the trade-offs.

Performance: We first examine through simulation the performance of a local model compared with that of the global model and commonly-used protocol models in the prior work [6][9][22].

A wireless network is generated with 50 randomly-positioned nodes, $\alpha = 4$, and $\text{SINR}_{th} = 20$. 10 simulations are conducted using random initial topologies and link activities, and the results are averaged. The interference range is the entire network for the global model, and chosen to be r_f=4 for the local model. The protocol model assumes a separation (i.e., contention) range of r_s without using an interference range.

Figure 8 shows the one-hop capacity achieved by the global model, the local model, and the protocol model, respectively. For r_s large, the protocol model fails to maximize the spatial channel-reuse. This is because the contention constraint is too stringent. For r_s small, the protocol model over-utilizes the channel resource, resulting in a violation of SINR constraint and a reduced spatial-reuse. Even at the optimal separation range (r_s=3) the spatial-reuse of the protocol model is less than that of the local model by 23%. The inefficient spatial-reuse is due to the protocol model that cannot take a non-circular contention region into consideration. On the contrary, the global and local models characterize the interference and non-circular contention regions and thus represent the neighborhood system of dipoles more accurately. Compared to the global model, the local model has 8% less spatial reuse on the average, showing the performance degradation of a simpler model.

We now examine the tightness of the bound on the approximation error. Specifically, the approximation error is measured from simulations and compared with that calculated from Theorem 1. A linear topology is selected, where 100 nodes are randomly placed and a node communicates with two neighbors. A linear topology is chosen as it provides a worst case of non-circular contention- and interference-regions. Other parameters used in the simulations are $\alpha = 4$, SINR_{th}=10, N=100, r_c=10, and a varying r_f to obtain values for $\mathcal{C}$.

Results are shown in Figure 9. The measured approximation error decreases sharply as $\mathcal{C}$ increases and is indeed bounded by $E(\Delta)$. The bound follows the same trend as the actual approximation error. The difference between the measured approximation error and the bound may result from the linear topology whose density of active links is much sparser than the assumptions in Theorem 1. Intersections between C and $E[\Delta]$ (or the bound) illustrate the performance-complexity trade-off.

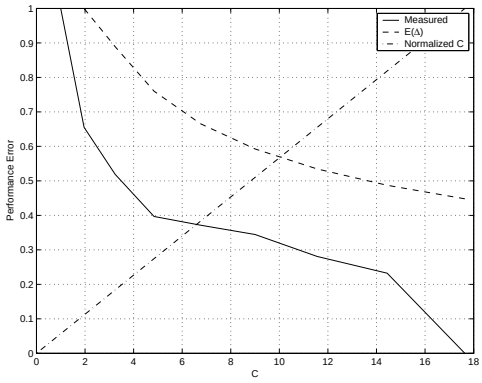

Fig. 9. Measured Approximation Error and Upper Bound $E(\Delta)$

Complexity: We now compare the communication complexity of a local and a global model through simulations. We use the same parameters and the number of runs in the simulation. The actual communication complexity is obtained by counting the number of the neighboring active links within the interference range of each active dipole, and averaged over all active dipoles and 10 runs. Figure 10 shows the communication complexity for both the global and local model as a function of network size N. The communication complexity of the centralized global optimization increases linearly with N since each node uses the information from all other nodes in the network. The complexity increases slowly with N for the distributed algorithm.

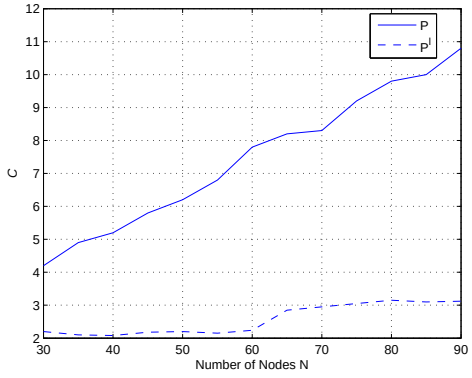

Fig. 10. Communication complexity $\mathcal{C}$ vs network size N. P and P^l: global and local model, respectively.

Extension: We now consider an extension to multiple time-slots to show the promise of the distributed algorithm to scheduling in a more realistic setting. This is motivated by the

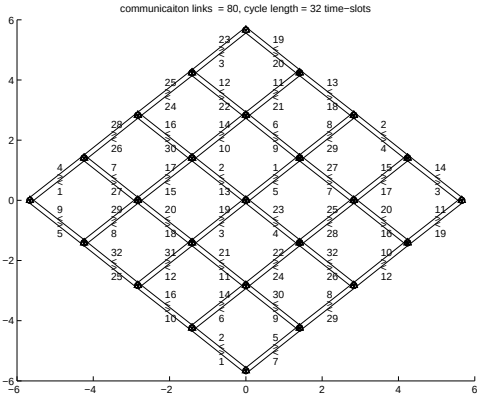

Fig. 11. Timeslot Allocation of Spatial Time Division Multiple Access (STDMA)

prior work [24] that shows optimal scheduling decisions can be done in a fully distributed fashion. [24] considers packet-level scheduling, the queue size and packet arrivals but a simplified interference model. Our model does not include packet arrivals and queue occupancy but uses a general interference model and adapts physical topology also. To compare these two works at a common ground, we assume that there is one queue for each communication link and a queue is always busy, and a physical topology is given. Our local probabilistic model is extended directly to include multiple time-slots in the coefficients and details are given in Appendix II. We conduct a simulation for scheduling using the following parameters: $\alpha = 4$, N= 25, l_{th}=2, and r_f=6 for regular topology in Figure 11. There are 80 links and 32 assigned time-slots. The figure shows that the optimal allocations are obtained in these examples by the local model and the distributed algorithm while satisfying the SINR constraints. Hence, compared with [24] when a physical topology is given, an advantage of the local model is its ability to approximate the general (non-Markovian) SINR model. A disadvantage of our local model is a lack of specifications of network traffic.

VIII. Conclusion

We have developed an analytical framework in which near-optimality, approximation and randomized distributed algorithms can be studied for self-configuration, i.e., joint configuration of a topology and scheduling. Our findings are summarized as follows.

(a) We begin with a global model that characterizes the ground truth in regard to network assumptions. The ground truth includes the randomness from a network internally and management constraints imposed externally. The resulting model is a Gibbs distribution where the exponent can be regarded as a cost function. This relates modeling with optimization so that both randomness in a network and objectives can be combined naturally. This approach differs from the pure "emerging behavior" where nodal decisions are not governed by an optimal performance. This approach also differs from the "black-box" method where models are learned externally.

A disadvantage of our approach is the simple assumptions that limit the current model. Fading has not been included

in our model. Traffic demands at network-layer have been considered in developing a probabilistic graphical model in [21] but not yet in this work.

(b) The mathematical representation of the global model quantifies the statistical spatial dependence of node positions and node-node communication. The complex spatial dependence is represented explicitly by a probabilistic graph. The graph shows how to obtain a local model to approximate the global model. The local model is a two-layer Markov Random Field or a random bond model. The complexity of the local model is the communication range of nodes from neighborhoods in the Markov Random Field. We remove long links in the graph to obtain a local model, and a more sophisticated approach may be explored to obtain a better approximation.

(c) We have derived sufficient conditions on the near-optimality of the local model under different channel conditions, density of nodes, network size and complexity. The conditions show a trade-off between the near-optimality and complexity. For example, a local model is near-optimal with a moderate complexity if a channel has a fast power decay of order at least 4; and may not be near-optimal, otherwise. The near-optimality conditions thus complement the empirical choices in protocol designs (e.g. 802.11), and may provide a practical utility in regard to the effect of channel attenuation, densities of nodes, and node-pair communications.

(d) Near-optimal local models render a class of randomized distributed algorithms for self-configuration. The algorithm allows each node to adapt probabilistically its local configuration using only information from neighbors. Local self-configuration collectively achieves a near-optimal global configuration. Also, the distributed algorithm achieves a near-optimal configuration at a bounded communication complexity. Hence the algorithmic advantage is a strength of the local model. We have shown examples of stochastic scheduling and reconfiguration upon failures, and compared the performance and complexity with existing protocol models.

One disadvantage of stochastic relaxation is the slow convergence that has been explored in the prior work [10]. Other simple randomized algorithms have been discussed in [20]. It would be beneficial to study simpler randomized algorithms.

APPENDIX

I. PROOF OF THEOREM 1

Proof: We begin proving the theorem by bounding the error, i.e., $|\frac{H(\boldsymbol{\sigma}^*|\boldsymbol{X})-H(\hat{\boldsymbol{\sigma}}|\boldsymbol{X})}{H(\boldsymbol{\sigma}^*|\boldsymbol{X})}| \leq \frac{|H(\boldsymbol{\sigma}^*|\boldsymbol{X})-H(\hat{\boldsymbol{\sigma}}|\boldsymbol{X})|^u}{|H(\boldsymbol{\sigma}^*|\boldsymbol{X})|^l}$, where the superscripts u and l denote an upper and a lower bound of the corresponding quantity.

To find an upper bound of the numerator, we have $|H(\boldsymbol{\sigma}^*|\boldsymbol{X}) - H(\hat{\boldsymbol{\sigma}}|\boldsymbol{X})| = |(H(\boldsymbol{\sigma}^*|\boldsymbol{X}) - H^l(\boldsymbol{\sigma}^*|\boldsymbol{X})) + (H^l(\hat{\boldsymbol{\sigma}}|\boldsymbol{X})) - H(\hat{\boldsymbol{\sigma}}|\boldsymbol{X}) + (H^l(\boldsymbol{\sigma}^*|\boldsymbol{X}) - H^l(\hat{\boldsymbol{\sigma}}|\boldsymbol{X}))| \leq |H(\boldsymbol{\sigma}^*|\boldsymbol{X}) - H^l(\boldsymbol{\sigma}^*|\boldsymbol{X})| + |H(\hat{\boldsymbol{\sigma}}|\boldsymbol{X}) - H^l(\hat{\boldsymbol{\sigma}}|\boldsymbol{X})|$, where the inequality holds since $H(\boldsymbol{\sigma}^*|\boldsymbol{X}) \leq H(\hat{\boldsymbol{\sigma}}|\boldsymbol{X})$, and $H^l(\hat{\boldsymbol{\sigma}}|\boldsymbol{X}) \leq H^l(\boldsymbol{\sigma}^*|\boldsymbol{X})$ by definition.

For any configuration $(\boldsymbol{\sigma}|\boldsymbol{X})$, $|H(\boldsymbol{\sigma}|\boldsymbol{X}) - H^l(\boldsymbol{\sigma}|\boldsymbol{X})| \leq |R_I(\boldsymbol{\sigma}|\boldsymbol{X})| + |R_3(\boldsymbol{\sigma}|\boldsymbol{X})|$. Let I_3 and I_R be an upper bound of $|R_3(\boldsymbol{\sigma}|\boldsymbol{X})|$ and $|R_I(\boldsymbol{\sigma}|\boldsymbol{X})|$, respectively, where

$$\begin{aligned}
|R_3(\boldsymbol{\sigma}|\boldsymbol{X})| &\leq \sum_{k_1=1}^{\frac{r_f}{r_c}} \sum_{k_2=1}^{\frac{r_f}{r_c}} 2P_t k_1^{\frac{-\alpha}{2}} k_2^{\frac{-\alpha}{2}} r_c^{-\alpha} \\
&\leq 2P_t \left(1 + (\int_{k=1}^{\frac{r_f}{r_c}} k^{\frac{-\alpha}{2}} dk)\right)^2 \cdot r_c^{-\alpha} \\
&= \begin{cases} 2P_t r_c^{-\alpha}(1 + 0.5 \ln \mathcal{C})^2, & \alpha = 2 \\ \frac{2P_t r_c^{-\alpha}}{(\alpha-2)^2}(\alpha - 2(\mathcal{C})^{\frac{2-\alpha}{2}})^2, & \alpha > 2 \end{cases} \\
&= I_3,
\end{aligned}$$

where "1" appears in the above expression to ensure that the discrete sum upper bounds the integral. The penalty term in the configuration Hamiltonian is not included as I_3 is an upper bound.

We now find I_R. Consider an active dipole σ_{ij}, and let G_k be the set of neighboring active dipoles that are $r_f + kr_c$ apart from the receiver. The cardinality of G_k is upper bounded, i.e., $|G_k| \leq \frac{2\pi}{\theta} = \pi / \sin^{-1}\left(\frac{\frac{r_c}{2}}{r_f+(k-1)r_c}\right) < 2\pi(r_f + (k-1)r_c)/r_c$.

For an active dipole σ_{ij}, let I_{kU} be an upper bound of the residual interference outside interference range[9], i.e.,

$$\begin{aligned}
R_{I_{ij}}(\boldsymbol{\sigma}|\boldsymbol{X}) &\leq \sum_{k=1}^{k_U} 2P_t 2\pi \cdot \frac{(r_f + (k-1)r_c)^{\frac{2-\alpha}{2}}}{r_c} (l_{th}(1+\epsilon_0))^{\frac{-\alpha}{2}} \\
&= I_{k_U},
\end{aligned}$$

where k_U is an integer that satisfies the inequality

$$\frac{(N-2)l_{th}(1+\epsilon_0)}{r_c} \leq \sum_{k=1}^{k_U} 2\pi \frac{r_f + (k-1)r_c}{r_c}. \tag{20}$$

The value $\frac{(N-2)l_{th}(1+\epsilon_0)}{r_c}$ denotes an upper bound of the maximum number of available active dipoles except σ_{ij} (with two nodes) in a network with total N nodes. k_U can be solved from the above inequality as $k_U \leq r_c + \sqrt{N l_{th} r_c}$. Using this bound for k_U and replacing r_f by $\sqrt{\mathcal{C}} r_c$, we have

$$\begin{aligned}
& I_{k_U} \\
\leq\ & \frac{2P_t 2\pi}{r_c (l_{th}(1+\epsilon_0))^{\frac{\alpha}{2}}} \left(r_f^{\frac{2-\alpha}{2}} + \int_1^{k_U^u} (r_f + (k-1)r_c)^{\frac{2-\alpha}{2}} dk \right) \\
\leq\ & \begin{cases} \frac{P_t 4\pi}{r_c^2 (l_{th}(1+\epsilon_0))^{\frac{\alpha}{2}}} \left(\frac{1}{\sqrt{\mathcal{C}}} + \ln(1 + \sqrt{N l_{th}/(\mathcal{C} r_c)}) \right), & \alpha = 4 \\ \frac{P_t 4\pi}{r_c^2 (l_{th}(1+\epsilon_0))^{\frac{\alpha}{2}}} \Big(\mathcal{C}^{\frac{2-\alpha}{4}} r_c^{\frac{4-\alpha}{2}} + \frac{2}{4-\alpha} \cdot \\ \left(-(\sqrt{\mathcal{C}} r_c)^{\frac{4-\alpha}{2}} + (\sqrt{\mathcal{C}} r_c + \sqrt{N l_{th} r_c})^{\frac{4-\alpha}{2}} \right) \Big), & \alpha \neq 4. \end{cases} \\
=\ & I_R.
\end{aligned}$$

Thus, $|H(\boldsymbol{\sigma}^*|\boldsymbol{X}) - H(\hat{\boldsymbol{\sigma}}|\boldsymbol{X})| \leq |H(\hat{\boldsymbol{\sigma}}|\boldsymbol{X}) - H^l(\hat{\boldsymbol{\sigma}}|\boldsymbol{X})| + |H(\boldsymbol{\sigma}^*|\boldsymbol{X}) - H^l(\boldsymbol{\sigma}^*|\boldsymbol{X})| \leq 2(I_R + I_3) N_{\sigma}{}^*$, where $N_{\sigma}{}^*$ is total number of active dipoles in $\boldsymbol{\sigma}^*$ given $\boldsymbol{X}$.

To obtain a lower bound for $|H(\boldsymbol{\sigma}^*|\boldsymbol{X})|$, we take only the net energy term in $H(\boldsymbol{\sigma}^*|\boldsymbol{X})$ as the penalty term is usually small, i.e., close to zero when the constraint is satisfied. Then $|H(\boldsymbol{\sigma}^*|\boldsymbol{X})| \geq \min\{P_t l_{ij}^{-\alpha} - \sum_{mn \neq ij} P_t l_{mj}^{\frac{-\alpha}{2}} l_{ij}^{\frac{-\alpha}{2}}\} N_{\sigma}^*$

[9] Similar to I_3, the penalty term is not included for deriving an upper bound.

for $\forall\ \sigma_{ij} = 1$. For $\sigma_{ij} = 1$, to satisfy a given SINR$_{th}$, a sufficient condition is $(P_t(\sum_{mn\neq ij} l_{mj}^{\frac{-\alpha}{2}})^2 + N_b)/(P_t(l_{ij}^{\frac{-\alpha}{2}})^2) \leq 1/\text{SINR}_{th}$, thus $(\sum_{mn\neq ij} l_{mj}^{\frac{-\alpha}{2}})^2 \leq (\frac{l_{ij}^{-\alpha}}{\text{SINR}_{th}} - \frac{N_b}{P_t})$. Therefore, $|H(\boldsymbol{\sigma}^*|\boldsymbol{X})| \geq (P_t l_{th}^{-\alpha}(l+\epsilon_0)^{-\alpha} - P_t l_{th}^{\frac{-\alpha}{2}}(l-\epsilon_0)^{\frac{-\alpha}{2}} \sqrt{l_{th}^{\frac{-\alpha}{2}}(1-\epsilon_0)^{\frac{-\alpha}{2}}\text{SINR}_{th}^{-1} - \frac{N_b}{P_t}})\ N_\sigma^*$.

Hence, $|\frac{H(\boldsymbol{\sigma}^*|\boldsymbol{X})-H(\hat{\boldsymbol{\sigma}}|\boldsymbol{X})}{H(\boldsymbol{\sigma}^*|\boldsymbol{X})}|] \leq \epsilon_\Delta$, where $\epsilon_\Delta = 2(I_R + I_3)/I_D$, $I_D = P_t l_{th}^{-\alpha}(l+\epsilon_0)^{-\alpha} - P_t l_{th}^{\frac{-\alpha}{2}}(l-\epsilon_0)^{\frac{-\alpha}{2}}\sqrt{l_{th}^{\frac{-\alpha}{2}}(1-\epsilon_0)^{\frac{-\alpha}{2}}/\text{SINR}_{th} - \frac{N_b}{P_t}}$.

Assume ϵ_0=0 for a simple representation,

$$\epsilon_\Delta = \begin{cases} \frac{\mathcal{I}}{r_c^2}\left((2+\ln\mathcal{C})^2 + \frac{4\pi}{l_{th}}(r_c+\sqrt{Nl_{th}r_c})\right), & \alpha=2 \\ \frac{\mathcal{I}}{r_c^2}\left(\frac{2(2-\frac{1}{\mathcal{C}})^2}{r_c^2} + \frac{4\pi}{l_{th}^2}(\frac{1}{\sqrt{\mathcal{C}}} + \ln(1+\sqrt{\frac{Nl_{th}}{\mathcal{C}r_c}}))\right), & \alpha=4 \\ \frac{\mathcal{I}}{r_c^2}\left(\frac{2(\alpha-2\mathcal{C}^{\frac{2-\alpha}{2}})^2}{(\alpha-2)^2 r_c^{\alpha-2}} + \frac{4\pi}{l_{th}^2}\left(\mathcal{C}^{\frac{2-\alpha}{4}} r_c^{\frac{4-\alpha}{2}} + \frac{2}{4-\alpha}(\right.\right. & \\ \left.\left. -(\sqrt{\mathcal{C}}r_c)^{\frac{4-\alpha}{2}} + (\sqrt{\mathcal{C}}r_c+\sqrt{Nl_{th}r_c})^{\frac{4-\alpha}{2}}\right)\right), & \text{o.w.,} \end{cases}$$

where $\mathcal{I}= 2/\left(l_{th}^{\frac{-\alpha}{2}}(l_{th}^{\frac{-\alpha}{2}} - \sqrt{l_{th}^{-\alpha}/\text{SINR}_{th} - N_b/P_t})\right)$.

Moreover, since the bounds derived above hold for any (σ, X), they also holds for the expected value, i.e., $E[|\frac{H(\boldsymbol{\sigma}^*,\boldsymbol{X}^*)-H(\hat{\boldsymbol{\sigma}},\hat{\boldsymbol{X}})}{H(\boldsymbol{\sigma}^*,\boldsymbol{X}^*)}|] \leq \epsilon_\Delta$.

II. Model Extension to Multiple Timeslots

As the slot allocation is based on the spatial dependence among neighboring nodes and links, we extend the local model and the distributed algorithm to spatial time division multiple access (STDMA). We assign a time slot S_{ij} to a dipole (i,j), $1 \leq S_{ij} \leq S_{max}$, where S_{max} is the TDMA cycle length. Since S_{max} is unknown, we then generalize the coefficients in the Hamiltonian in (6) as functions of time slots,

$$\begin{aligned} \alpha_{ij}^{'} &= \alpha_{ij}\cdot\omega_s(S_{ij}), \\ \alpha_{ij,mn}^{'} &= \alpha_{ij,mn}\delta(S_{ij},S_{mn})\cdot\omega_s(S_{ij}) \\ \alpha_{ij,mn,uv}^{'} &= \alpha_{ij,mn,uv}\delta(S_{ij},S_{mn})\delta(S_{ij},S_{uv})\cdot\omega_s(S_{ij}), \end{aligned} \tag{21}$$

where S_{ij} is the time-slot number of TDMA cycle for dipole (i,j), and $\delta(S_{ij},S_{mn})$=1 if $S_{ij}=S_{mn}$; $\delta(S_{ij},S_{mn})$=0, otherwise. $\omega_s(S_{ij})$ is a function that is inverse-proportional to S_{ij}, and $\omega_s(S_{ij}) = \frac{1}{S_{ij}}$ is used in this work. This enables early sequences of timeslots to play an more important role in minimizing the potential energy. For example, the first timeslot is utilized first and so on. As a result, the length of STDMA cycle S_{max} is minimized.

The resulting MRF model is now defined over multiple orthogonal time slots, i.e. S_{max} time slots, and a communication dipole σ_{ij} now takes an extended form of $\sigma_{ij}\cdot\delta(\boldsymbol{S}_{ij}-s)$, where $\delta(\boldsymbol{S}_{ij}-s)$=1 if $\boldsymbol{S}_{ij}$=s; 0, otherwise, for $1\leq s\leq S_{max}$.

Acknowledgement

The authors gratefully acknowledge the support from NSF ECS 0300605 and ECS 990857. The authors would like to thank anonymous reviewers for helpful comments. C.Ji would like to thank C.S. Ji and J. Modestino for helpful discussions on Markov Random Fields.

References

[1] J. Baras, and X. Tan, *"Control of Autonomous Swarms Using Gibbs Sampling,"* In Proc. of *IEEE CDC*, vol. 5, pp. 4752-4757, Dec. 2004.

[2] P. Bjorklund, P. Varbrand, and D. Yuan, *"Resource Optimization of Spatial TDMA in Ad Hoc Radio Networks: A Column Generation Approach,"* In Proc. Of *IEEE Infocom*, vol. 2, pp. 818-824, April 2003.

[3] M. Chiang, *"Distributed Network Control Through Sum Product Algorithm on Graphs,"* In Proc. of *IEEE Globecom*, vol. 3, pp. 2395-2399, Nov. 2002.

[4] T. Elbatt, and A. Ephremides, *"Joint Scheduling and Power Control for Wireless Ad Hoc Networks," IEEE Trans. Wireless Communications*, vol. 3, pp.74-85, Jan. 2004.

[5] D. Estrin, R. Govindan, J. Heidemann, and S. Kumar, *"Next Century Challenges: Scalable Coordination in Sensor Networks,"* In Proc. of *ACM Mobicom*, pp. 263-270, Aug. 1999.

[6] S. Gandham, M. Dawande, and R. Prakash *"Link Scheduling in Sensor Networks: Distributed Edge Coloring Revisited,"* In Proc. of *IEEE Infocom*, vol. 4, pp. 2492-2501, Mar. 2005.

[7] S. Geman, and D. Geman, *"Stochastic Relaxation, Gibbs Distributions, and the Bayesian Restoration of Images," IEEE Trans. PAMI*, vol.6, pp.721-741, June 1984.

[8] M. Greiner, *" Self-organizing control of network structure in wireless communication,"* In Proc. of *IMA Wireless Communications Workshop*, June 2005.

[9] P. Gupta, and P.R. Kumar, *"The Capacity of Wireless Networks," IEEE Trans. Information Theory*, vol. 46, no. 2, pp. 388-404, Mar. 2000.

[10] B. Hajek and G. Sasaki, *"Link Scheduling in Polynomial Time," IEEE Trans. Information Theory*, Vol.34, No.4, Sept. 1988.

[11] J. Hromkovic, R. Kralovic, M. Nunkesser, and P. Widmayer, *" Randomized Algorithms and Probabilistic Analysis in Wireless Networking,"* In Proc. of*Symposium on Stochastic Algorithms, Foundations, and Applications*, LNCS 4665, Springer, pp. 54-57, 2007.

[12] K. Huang, *"Statistical Mechanics," John Wiley & Sons*.

[13] S. Jeon and C. Ji, *"Nearly Optimal Distributed Configuration Management Using Probabilistic Graphical Models,"* In Proc. of *IEEE MASS, RPMSN workshop*, pp. 1-8, Nov. 2005.

[14] S. Jeon, *"Near-Optimality of Distributed Network Management with a Machine Learning Approach," http://smartech.gatech.edu/dspace/handle/1853/16136, Ph.D Thesis*, July 2007.

[15] M. Jordan, and Y. Weiss, *"Graphical Models: Probabilistic Inference," Handbook of Neural Networks and Brain Theory*, 2002.

[16] B. Kauffmann, F. Baccelli, A. Chaintreau, V. Mhatre, D. Papagiannaki, and C. Diot, *"Measurement-based self organization of interfering 802.11 wireless access networks,"* In Proc. of *IEEE Infocom*, 2007.

[17] F. Kschischang, B. Frey, H. Loeliger *"Factor graphs and the sum-product algorithm," IEEE Trans. on Information Theory*, vol. 47, no. 2, pp. 498-519, Feb. 2001.

[18] B. Ko, and D. Rubenstein, *"A Distributed, Self-stabilizing Protocol for Placement of Replicated Resources in Emerging Networks,"* In Proc. of *ACM ICNP*, pp. 6-15, Nov. 2003.

[19] S. Z. Li, *"Markov Random Field Modeling in Computer Vision," Springer-Verlag*.

[20] X. Lin, N. Shroff and R. Srikant, *"A Tutorial on Cross-Layer Optimization in Wireless Networks," IEEE Journal of Selected Areas of Communication*, vol.24, Issue 8, pp.1452-1463, June 2006.

[21] G. Liu, and C. Ji, *"Cross-Layer Graphical Models for Resilience of All-Optical Networks under Crosstalk Attacks," IEEE JSAC Optical Communications and Networking Series*, vol. 25, pp. 2-17, 2007.

[22] H. Luo, S. Lu, V. Bharghavan, J. Cheng, and G. Zhong, *"A Packet Scheduling Approach to QoS Support in Multihop Wireless Networks," ACM MONET*, vol. 9, no. 3, pp. 193-206, June 2004.
[23] R. Madan, S. Cui, S. Lall, and A. Goldsmith, *"Cross-Layer Design for Lifetime Maximization in Interference-Limited Wireless Sensor Networks" IEEE Trans. Wireless Communications*, vol. 5, No. 11, pp. 3142-3152, Nov. 2006.
[24] E. Modiano, D. Shah, and G. Zussman, *" Maximizing Throughput in Wireless Networks via Gossiping,"* In Proc. of *ACM SIGMETRICS / IFIP Performance* , Jun. 2006.
[25] K. Oikonomou and I. Stavrakakis, "Analysis of Topology-Unaware TDMA MAC Policies for Ad-Hoc Networks Under Diverse Traffic Load," *ACM Mobile Computing and Communications Review, special issue on Medium Access and Call Admission Control Algorithms for Next Generation Wireless Networks*, Vol. 9, pp. 25-38. Oct. 2005
[26] G. Pottie, and W. Kaiser, *"Wireless integrated network sensors," Communications of the ACM*, vol. 43. no. 5, May 2000.
[27] T. Rappaport, *"Wireless Communications: Principles and Practice," Prentice Hall*.
[28] W. Spears, D. Spears, J. Hamann, and R. Heil, *"Distributed, Physics-Based Control of Swarms of Vehicles," Kluwer Autonomous Robots*, vol. 17, pp. 137-162, Aug. 2004.
[29] A. Srinivasan, and A. Panconesi, *"Fast Randomized Algorithms for Distributed Edge Coloring,"* In Proc. of *ACM Symposium on Principles of Distributed Computing* , pp. 251-262, 1992.
[30] M. Steenstrup, *"Emergent Structure Among Self-Organizing Devices,"* In Proc. of *NSF-RPI Workshop on PCN*, April 2004.
[31] J. Tsitsiklis and M. Athens, *" On the Complexity of Decentralized Decision Making and Detection Problem," IEEE Trans. Automatic Control* , vol. 30, no. 5, pp.440-446, May 1985.
[32] A. Wagner, and V. Anantharam, *" Wireless sensor network design via interacting particles,"* In Proc. of *Allerton*, Oct. 2002.
[33] R. Wattenhofer, L. Li, P. Bahl, and Y. Wang, *"Distributed topology control for power efficient operation in multihop wireless networks,"* In Proc. of *IEEE Infocom*, vol. 3, pp. 1388-1397, April 2001.

PLACE PHOTO HERE

Sung-eok Jeon received the B.S. degree from Yonsei University, Seoul, Korea, in 1996, the M.S. degree from KAIST, Daejeon, Korea, in 1999, the Ph.D degree from Georgia Institute of Technology, in 2007, all in Electrical Engineering. He is now in Microsoft. His research interests are in statistical distributed management of large and complex networks, based on the probabilistic graphical models.

PLACE PHOTO HERE

Chuanyi Ji 's research lies in the areas of networking, machine learning, and their interfaces. Her research interests are in understanding and managing complex networks, applications of machine learning to network management and security, large-scale measurements, learning theory and algorithms, and information theory. Chuanyi Ji received the B.S. (Honors) degree from Tsinghua University, Beijing, China, in 1983, the M.S. degree from the University of Pennsylvania, Philadelphia, in 1986, and the Ph.D. degree from the California Institute of Technology, Pasadena, in 1992, all in electrical engineering. She is an Associate Professor in the Department of Electrical and Computer Engineering, Georgia Institute of Technology, Atlanta. She was on the faculty at Rensselaer Polytechnic Institute, Troy, NY, from 1991 to 2001. Chuanyi Ji received an NSF Career Award in 1995, and an Early Career Award from Rensselaer Polytechnic Institute in 2000.